Staggered magnetic susceptibility in high-T_c systems: A scaling approach

P. E. Engelstad* and K. Yamada
Department of Physics, Kyoto University, Kyoto 606-01, Japan
(Received 27 March 1995)

A scaling theory is applied in order to calculate the temperature dependence of the staggered magnetic susceptibility associated with the antiferromagnetism observed in high-temperature superconductors. In a logarithmic approximation, only a summation of the leading square logarithmic terms are taken into account, assuming the parquet approximation. We show that scaling theory can be applied to the square logarithmic two-dimensional problem. The scaling method is an improvement compared to the alternative random-phase approximation method. Our scaling result explains the temperature and doping dependence of the nuclear-spin-lattice relaxation time observed in high-T_c systems to satisfaction. However, the results of this paper indicate that the logarithmic parquet approximation may not be sufficient to calculate quantitatively the magnetic susceptibility. Ways to improve the theory are discussed.

I. INTRODUCTION

The scaling theory has so far been applied to high-T_c systems only to examine the transition temperatures required for the formation of ordered states.[1,2] This paper develops this idea further and goes on to calculate temperature dependencies of the correlation functions in the normal state in general. This approach may lead to a better picture of the unusual magnetic properties observed in high-T_c systems, in particular $La_{2-x}Sr_xCuO_{4-\delta}$ (LSCO). The temperature dependence of the staggered magnetic susceptibility in LSCO will be calculated and compared to experimental results.

The scaling theory developed in this paper reproduces the standard random-phase-approximation (RPA) expression only when the summation of ladder diagrams is taken into account. In that sense, the scaling method is an improvement compared to the RPA method. The strength of the scaling approach is that it takes the summation of both the electron-electron and the electron-hole diagrams into account.

The starting point is a half-filled band case. The model may also picture high-T_c systems which are more heavily doped than LSCO, e.g., systems like $Tl_2Ba_2CuO_{6+\delta}$ (TBCO) and $YBa_2Cu_3O_{7-\delta}$ (YBCO). The temperature-independent behavior of the staggered magnetic susceptibility at low temperatures and high doping values can be explained qualitatively from the chemical potential, which is taken to be a low-energy cutoff parameter. The chemical potential gives the Fermi energy shift from the half-filling due to doping.

The validity of the scaling approach is justified when the results are compared to experimental results. The results of our approach give Curie-Weiss behavior of the staggered magnetic susceptibility. With reasonable values for the parameters t and U/t, reasonable values for Weiss temperatures and Curie constants are obtained (t is the intersite transfer integral and U is the Coulomb repulsion on the Cu site).

II. THE 2D HUBBARD MODEL

The physical model focuses on repulsive interactions between electrons close to the van Hove singularities. It is described on the basis of the two-dimensional (2D) Hubbard model

$$H=-t\sum_{i,j,\sigma}(a^{\dagger}_{i,\sigma}a_{j,\sigma}+a^{\dagger}_{j,\sigma}a_{i,\sigma})+\frac{U}{2}\sum_i n_i n_i-\mu\sum_i n_i, \tag{1}$$

where $a^{\dagger}_{i,\sigma}(a_{i,\sigma})$ is the creation (destruction) operator of an electron on the Cu site i with spin projection $\sigma=\uparrow$ or $\sigma=\downarrow$. The operator n_i is defined as $n_i=n_{i,\uparrow}+n_{i,\downarrow}$, where $n_{i,\sigma}$ is the number operator $n_{i,\sigma}=a^{\dagger}_{i,\sigma}a_{i,\sigma}$. The second term in (1) contains the potential term $Un_i/2$. We consider that this term and the site-diagonal term $\varepsilon_0 n_i$ are included in the chemical potential μ and μ is assumed to be independent of U by choosing ε_0 as a proper function of U so as to fix the number of electrons. Thus, the Hamiltonian does not distinguish between the spin of the scattering particles. When considering the half-filled band case ($\mu=0$), the dispersion relation

$$\epsilon_k=-2t(\cos k_x+\cos k_y) \tag{2}$$

gives a perfectly nested, square Fermi surface. The saddle points, exactly at its corners, give rise to the van Hove singularity points with the density of states $N(\epsilon)=(1/2\pi^2 t)\ln(\pi^2/|\epsilon|)$. μ will change when the doping rate x in LSCO changes. Later in the paper the consequences of a nonzero, but nevertheless small value of μ will be discussed.

A correct treatment should take the full structure of Cu and O atoms present in the layer into account. The situation with Cu $d_{x^2-y^2}$ orbitals forming a lattice where the O p_σ orbitals connect to the nearest-neighbor Cu sites is well described with the d-p Hamiltonian. The d-p model, as treated by Kohno and Yamada,[3] gives rise to the energy bands

$$E^{\pm}_k=(\epsilon_d+\epsilon_p)/2 \pm\sqrt{(\epsilon_d-\epsilon_p)^2/4+2t^2_{d-p}(2-\cos k_x-\cos k_y)}-\mu. \tag{3}$$

If the upper d band ($\epsilon_d>\epsilon_p$) is the half-filled this dispersion relation can essentially be written in the form (2) and the

results described in this paper can be used when the d-p model is considered as well. This point can be understood as follows: At the half-filled case the Fermi surface is given by $\cos k_x+\cos k_y=0$ in (3). That is, $E^+_{k=k_F}=0$, where $k_y=\pm\pi-k_x$ or $k_y=\pm\pi+k_x$. As k deviates from k_F by a small value, E^+_k behaves as a linear function of $\cos k_x+\cos k_y$.

A upper energy cutoff E_c is introduced which restricts the momentum of the scattering particles. This region is divided into four branches, each one associated with one of the four singularity points in the corners of the Fermi surface. The momentum differences of $[2\pi,0]$ and $[0,2\pi]$ reduce the four points to a set of two equivalent points A and B. Thus, the 2D problem is reduced to a 1D-like problem with two cutoff branches, branch A and branch B.

In addition to the "symmetry" of the equivalent points, a 90° rotational symmetry in the layer is considered. This reduces the number of different types of scattering process between the branches to a number of four. The scattering processes $(A,A)\rightarrow(A,A)$, $(A,B)\rightarrow(B,A)$, $(A,A)\rightarrow(B,B)$, and $(A,B)\rightarrow(A,B)$ are associated with the couplings G_2, G_1, G_3, and G_4, respectively.

The unperturbed susceptibilities of the electron-hole bubble diagram $\chi^{(0)}(q,\omega)$ and the electron-electron bubble diagram $\Pi^{(0)}(q,\omega)$ will be calculated (q is the momentum transfer whereas ω is the frequency transfer). Thus, after introducing a cutoff $E_c=\pi^2 t$:

$$\Pi^{(0)}(q,\omega)=-\sum_{k'}\frac{1-f(\epsilon_{k'})-f(\epsilon_{-k'+q})}{-\omega+\epsilon_{k'}+\epsilon_{-k'+q}}\approx-\frac{1}{8\pi^2 t}\ln^2\frac{\omega}{E_c}, \tag{4}$$

$$\chi^{(0)}(q,\omega)=\sum_{k'}\frac{f(\epsilon_{k'+q})-f(\epsilon_{k'})}{-\omega+\epsilon_{k'}-\epsilon_{k'+q}}\approx\frac{1}{8\pi^2 t}\ln^2\frac{\omega}{E_c}. \tag{5}$$

The approximation marks above follow from the parquet approximation $[U/4\pi t\ll 1$, $(1/2\pi)\ln^2(\omega/E_c)\gg 1$, and $(U/8\pi^2 t)\ln^2(\omega/E_c)\sim 1]$ which implies that only square logarithmic terms should be taken into account. The main contribution to $\Pi^{(0)}(q,\omega)$ appears from the situation with inversion symmetry $q=[0,0]$, i.e., when $\omega\rightarrow 0$ and $\epsilon_{k'}=\epsilon_{(-k'+[0,0])}$ in the denominator of (4). Similarly, the nesting of the Fermi surface $q=[\pm\pi,\pm\pi]$, produces the main contribution to $\chi^{(0)}(q,\omega)$ in Eq. (5). All other terms can be neglected.

From the second-order spin-density wave (SDW) response diagram it can easily be seen that the staggered magnetic susceptibility $\chi([\pm\pi,\pm\pi],\omega)=\chi(\omega/E_c)$ can be written

$$\chi\left(\frac{\omega}{E_c}\right)=\frac{2}{U}\left[X\left(\frac{\omega}{E_c}\right)+(g_3+g_4)X^2\left(\frac{\omega}{E_c}\right)+\cdots\right], \tag{6}$$

where the dimensionless couplings g_i are defined by $g_i=G_i/U$ and the dimensionless response function X is defined by

$$X(\omega/E_c)=U\chi^{(0)}([\pm\pi,\pm\pi],\omega)=-U\Pi^{(0)}([0,0],\omega)$$
$$=(U/8\pi^2 t)\ln^2(\omega/E_c).$$

Finally, we define a function $\hat{\chi}(\omega/E_c)$ as

$$\hat{\chi}\left(\frac{\omega}{E_c}\right)=\frac{U}{2}\frac{\partial\chi[X(\omega/E_c)]}{\partial X(\omega/E_c)}=1+2(g_3+g_4)X\left(\frac{\omega}{E_c}\right)+\cdots. \tag{7}$$

With good approximation, ω can be replaced by $\max(\omega,2T,\mu)$. In other words, the integration of energy is stopped by the largest of these terms. In the case where the chemical potential $\mu\gg(\omega,2T)$, this is not completely true. μ will break the perfect nesting condition and reduce the square logarithmic terms of the electron-hole diagrams to single logarithms $\sim\ln\mu\ln T$. However, the electron-hole diagrams are the most important diagrams to consider, as far as the staggered magnetic susceptibility is concerned. Therefore, in the case of this paper, where only the leading square logarithmic terms will be taken into account, we assume the function $\max(\omega,2T,\mu)$ to be a reasonable approximation which can give a qualitative explanation of the experiments. In reality, the susceptibility will smoothly become constant as the temperature is reduced below the chemical potential. Thus, a function $\max[\omega,\sqrt{(2T)^2+\mu^2}]$ can be introduced to simulate this situation.

III. THE SCALING THEORY

It is necessary to go back to the simple formulation made by Anderson[4] to reveal the physics behind a scaling approach with leading square logarithmic terms. The cutoff can be reduced from E_1 to $E_2=E_1-\Delta E$. The cutoff works like a temperature scale and if the temperature is reduced correspondingly the required change in the couplings which keeps the physics unchanged can be found.

Thus, in the single logarithmic case with constant density of states, it is only the scattering processes with intermediate-state particles within the small region ΔE which will modify the Hamiltonian. These states are given by $\ln E_1/D-\ln E_2/D(\sim\Delta E/E)$ where D is a natural cutoff.

On the contrary, in the square logarithmic case it is the terms

$$X(E_1/D)-X(E_2/D)\sim\ln^2 E_1/D-\ln^2 E_2/D[\sim\rho(E)\Delta E/E],$$

which is responsible for the change of the couplings.

In the multiplicative renormalization the term $\ln E_1/E_2$ modifies the Hamiltonian. This is correct in the 1D case. However, in the 2D case, as long as the natural cutoff correctly is taken into account, we can use the formalism of the multiplicative renormalization using the simple substitution

$$\ln y=X\left(\frac{\omega}{E_c}\right), \tag{8}$$

where y is used for renormalization rather than ω/E_c. All the square logarithmic terms [$\ln^2(\omega/E_c)$, $\ln^4(\omega/E_c)$, . . . etc.] are transformed to single logarithmic ones.

Using reasonable physical arguments, the scaling theory should not be restricted to the case of single logarithmic terms with a constant density of states. Mathematically, in the original formulation by Bogoliubov and Shirkov[5] logarithmic terms were not a prerequisite. The validity of applying the multiplicative renormalization-group theory can only be justified or falsified by perturbational calculation. This is left for future work.

Following the procedure of multiplicative renormalization,[6,7] using substitution (8), it is straightforward to derive the well-known scaling equations

$$\partial g_1/\partial X=-2g_1(g_1-g_4),$$
$$\partial g_3/\partial X=-2g_3(g_2+g_1-2g_4), \tag{9}$$

$$\partial g_2/\partial X=-(g_2)^2-(g_3)^2, \quad \partial g_4/\partial X=(g_4)^2+(g_3)^2. \tag{10}$$

Using the same procedure for $\hat{\chi}$[6], we obtain the response equation

$$\frac{\partial}{\partial X}\ln\left(\frac{U}{2}\frac{\partial\chi(X)}{\partial X}\right)=2[g_3^R(X)+g_4^R(X)](=2\Gamma_{\rm SDW}). \tag{11}$$

Similar treatment can be carried out for all the responses SDW, charge-density wave, etc. Thus, the transition temperature and the broken symmetry can easily be examined from the second-order response diagrams and the scaling equations. In this paper we go further than exploring transition temperatures. We intend to find temperature dependencies in general.

The scaling equations were found by Schulz[1] who mainly emphasized the Poor man's scaling approach and by Dzyaloshinskii[2] who applied the Sudakov method to sum up all the parquet diagrams. It is believed that the response differential equation (11) also can be verified by a skeleton graph technique.

An interesting feature of this set of equations is that they are able to reproduce the standard RPA result. First, the scaling equations can be modified to sum up all the ladder diagrams. If only the second-order diagrams with crossed lines (i.e., second-order ladder diagrams or ladder diagrams with two steps) of the vertex are taken into account, while all the other electron-electron and electron-hole diagrams are neglected, the scaling equations concerning the staggered magnetic susceptibility are reduced to

$$\partial g_3^{\rm RPA}/\partial X=2g_3^{\rm RPA}g_4^{\rm RPA}, \tag{12}$$

$$\partial g_4^{\rm RPA}/\partial X=(g_3^{\rm RPA})^2+(g_4^{\rm RPA})^2. \tag{13}$$

Thus, by solving these trivial equations the correct sum of ladder diagrams is represented by

$$\Gamma_{\rm SDW}^{\rm RPA}=g_3^{\rm RPA}(X)+g_4^{\rm RPA}(X)=\frac{2}{1-2X}. \tag{14}$$

Finally using the response differential equation and performing straightforward integration, the correct RPA result is given

$$\chi^{\rm RPA}(X)=\frac{2X/U}{1-2X}=\frac{\chi^{(0)\rm RPA}}{1-U\chi^{(0)\rm RPA}}. \tag{15}$$

In Fig. 1 the RPA result $\chi^{\rm RPA}(X)$ is compared to the improved scaling result $\chi(X)$.

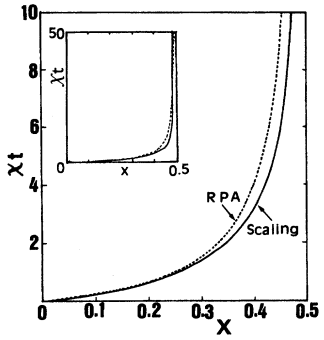

FIG. 1. The scaling method gives an improved result for the staggered magnetic susceptibility compared to the RPA-like summation of only ladder diagrams. $X=(U/8\pi^2t)\ln^2(2T/\pi^2t)$.

IV. COMPARISON OF THEORETICAL AND EXPERIMENTAL RESULTS

Kohno and Yamada[3] demonstrated that

$$\frac{1}{T_1T}\propto\chi([\pi,\pi],T) \tag{16}$$

for the case of strong antiferromagnetic fluctuations. T_1^{-1} is the nuclear-spin relaxation rate of ^{63}Cu. In $La_{2-x}Sr_xCuO_{4-\delta}$ (LSCO) T_1^{-1} has been thoroughly examined by Kitaoka *et al.*[8] using materials with a Sr content of $x=0.075$, $x=0.1$, $x=0.13$, $x=0.15$, and $x=0.20$. The experimental results are shown in Fig. 2.

According to Fig. 2 and Eq. (16), the staggered magnetic susceptibility will follow a Curie-Weiss law:

$$\chi([\pi,\pi],T)=\frac{C}{T+\Theta} \tag{17}$$

within a temperature range of 75–300 K.

This experiment further showed that the Weiss temperature Θ is proportional to the Sr content x, with the value of $\Theta\approx100$ K for $x=0.20$. Kitaoka *et al.*[8] linearly extrapolated

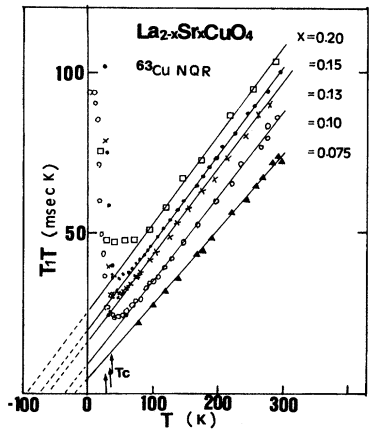

FIG. 2. The relaxation rate T_1^{-1} measured in LSCO. The data points are quoted from Kitaoka *et al.* (Ref. 8).

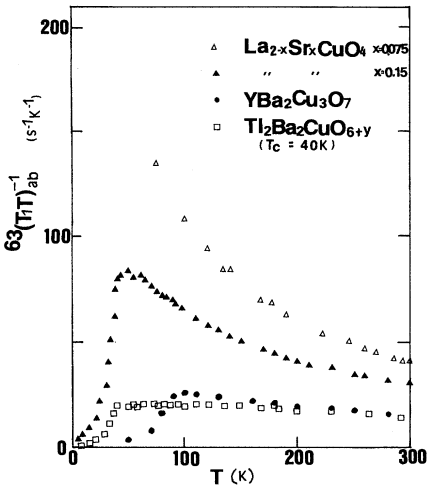

FIG. 3. The relaxation rate T_1^{-1} measured in LSCO, YBCO, and TBCO. The data points are quoted from Kitaoka *et al.* (Ref. 8).

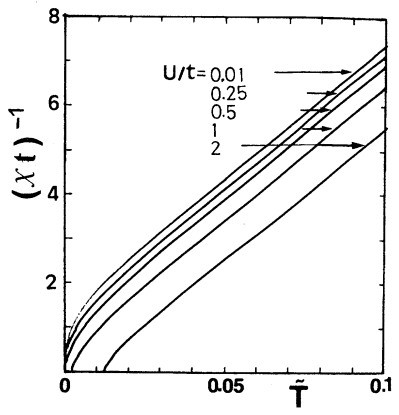

FIG. 4. The inverse of the staggered magnetic susceptibility is plotted as a function of the dimensionless temperature $\tilde{T}=2T/(4\pi^2 t)$ for different choices of U/t.

the Weiss temperatures as a function of doping and deduced that for the critical value where $\Theta=0$, the Sr content would be $x=0.05$.

Thus, larger x values correspond to lower staggered magnetic susceptibility as shown in the experiment for LSCO. Figure 3 reveals that the staggered magnetic susceptibility is lower in YBCO and TBCO than in LSCO. This is consistent with the fact that both YBCO and TBCO are heavily doped systems.

In Fig. 3 the effects of the cutoff factor μ, described in Sec. II, is illustrated. μ is expected to increase when the doping increases [Eq. (21)]. For the overdoped materials YBCO and TBCO, the cutoff factor seems to be large (approximately 200 K), resulting in the $(T_1T)=$const law. Above this temperature, the temperature dependence of the staggered magnetic susceptibility can be difficult to find due to the high Weiss temperatures that occur in systems with such high doping. On the contrary, LSCO is lightly doped, hence the cutoff factor μ is small. The staggered magnetic susceptibility is not constant for temperatures higher than 75 K.

V. COMPARISON OF SCALING CALCULATIONS TO EXPERIMENTAL RESULTS

First, t needs to be estimated to give the temperature scale of our result. A realistic value for t is expected to be in the region of 10^3–10^4 K. In this paper this parameter is chosen so that $2/(\pi^2 t)\approx 1/5t\approx 10^{-4}$ K^{-1}. Hence, the logarithmic term is approximately

$$\ln^2\frac{2T}{\pi^2 t}\approx\ln^2\frac{T}{10\,000\ \text{K}}. \tag{18}$$

A. The Curie-Weiss behavior

The inverse of the staggered magnetic susceptibility as predicted by the scaling theory is plotted in Fig. 4, as a variable of the dimensionless temperature $\tilde{T}=2T/\pi^2 t \approx T/10\,000$ K and for different choices of U/t ($U/t=2$, $U/t=1$, $U/t=0.5$, $U/t=0.25$, and $U/t=0.01$). Initially, this paper focused on weak correlations. However, a more realistic value is $U/t\approx 1\sim 2$. Therefore, the curve where $U/t=2$ is examined, despite the fact that the weak-coupling condition $U/(4\pi t)\ll 1$ is doubtful in this case. The curves with unrealistic low values of U/t ($U/t=0.25$ and $U/t=0.01$) are also plotted, because they give a good illustration of the analytical behavior of the curves when U/t changes.

Figure 4 shows that the magnetic susceptibility is close to the expected Curie-Weiss dependence shown in Fig. 2, and that all the curves are parallel using different choices of U/t. This is similar to the experimental curves. At low temperatures the staggered magnetic susceptibility diverges for a large value of U/t. This fact means that the antiferromagnetic instability occurs at this temperature. If this critical temperature is lower than the chemical potential μ, the temperature T should be replaced by μ within our scaling theory. This point will be discussed in Sec. V B.

Good linear fits to the curves of the inverse of the susceptibility shown in Fig. 4 are achieved when

$$\chi^{-1}\approx\frac{4\pi^2 t}{27}\left[2e^3\left(\frac{2T}{\pi^2 t}\right)+1\right]-D\times U,\quad D\approx 0.95. \tag{19}$$

These fits are found by linearlizing around the point where the curvature is zero, as illustrated in Fig. 5. The figure shows that the linearity breaks down at low temperatures close to the instability point. At high temperatures (outside the temperature range present in Fig. 5) the *inverse* of the staggered magnetic susceptibility gradually grows larger than the linear fits.

These linear fits show that with the quite realistic temperature scale choice in (17) the Weiss temperature will vary between $\Theta=100$ K and $\Theta=0$ K for $U/t\approx 1$ and $U/t\approx 1.5$. In other words, we can obtain reasonable values for the Weiss temperatures when reasonable values of U/t are used.

The cases where low values of x are used (Fig. 2) correspond to the curves with large values of U/t in Fig. 4. This tendency is exactly what is expected. The lightly doped system has strong correlations and the heavily doped system has

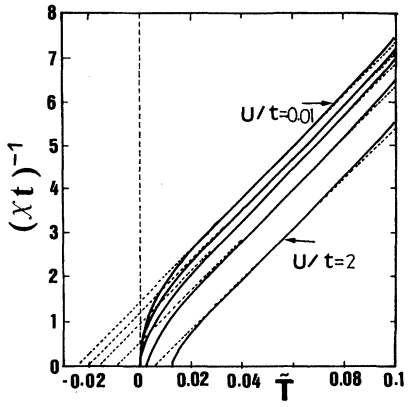

FIG. 5. Linear fits to the inverse of the staggered magnetic susceptibility. Linear fits where $\chi^{-1} \approx (4\pi^2 t/27)[2e^3(2T/\pi^2 t)+1]-0.95U$ has been used.

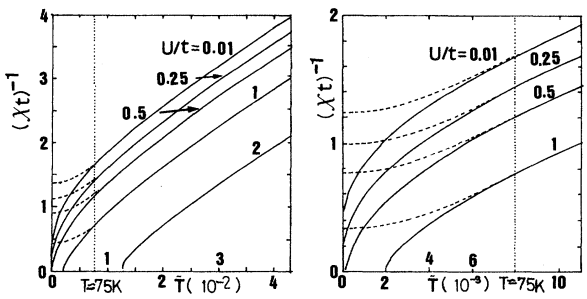

FIG. 6. The inverse of the staggered magnetic susceptibility is plotted for low temperatures. The different plots show the inverse of the magnetic susceptibility on different temperature scales. The broken lines show how the cutoff parameter μ can suppress the susceptibility, e.g., when $T \lesssim 75$ K.

weak correlations due to screening effects. [Thus, YBCO and TBCO are weak correlation systems whereas the undoped LSCO (La_2CuO_4) system has strong correlations.] If the scaling curves are correct, the doping and the correlation will be linearly related:

$$(x-a) \propto (b-U/t), \quad a,b=\text{const.} \tag{20}$$

It should be noted that in this linear area the RPA expression from Eq. (15) gives similar fits when D is set to unity, which means that the linear line is taken within a small interval on the X axis of Fig. 1. The small difference between the two curves can indicate that the electron-electron and electron-hole diagrams apart from the ladder diagrams will cancel each other out to such a great extent that the main contributions come from the ladder diagrams. If this is correct, it can justify the modified RPA method by self-consistent renormalization done by Moriya, Takahashi, and Ueda.[9]

It can also indicate that X is so small that the main contribution to the susceptibility comes from only lower order diagrams. These points are of great importance and should be examined closer.

B. $\mu \neq 0$

The order magnitude of the chemical potential μ can roughly be estimated as function of the doping value x:

$$x \approx \frac{1}{\pi^2 t}\int_{-\mu}^{0} \ln\frac{\pi^2 t}{|\epsilon|}\,d\epsilon = \frac{\mu}{\pi^2 t}\left(-\ln\frac{\mu}{\pi^2 t}+1\right). \tag{21}$$

Using the critical doping value $x=0.05$ which leads to zero Weiss temperature, Eq. (21) gives $\mu \approx 0.02$ eV, i.e., the susceptibility becomes constant when $T \lesssim 100$ K. This rough estimate is a little bit too high according to Fig. 3. It is more realistic to assume that the staggered magnetic susceptibility smoothly becomes constant when, e.g., $T<75$ K. (This is also quite a high value.) This situation is shown in Fig. 6.

The instability of the curve with $U/t=2$ does not disappear since the instability occurs at a temperature higher than 75 K (in our rough example). This curve can explain why neutron-scattering experiments[10] observe an instability in the staggered magnetic susceptibility in the close to undoped systems of LSCO. In these systems the doping is so low that the chemical potential μ cannot suppress the instability.

The cutoff factor μ is very roughly estimated, but it is clear that it will quickly increase when the doping increases. For the highly doped TBCO and YBCO, μ can easily become so large that it can explain the $(T_1T)=$const law observed in experiments. For even higher temperatures TBCO and YBCO are expected to show relatively low values for the staggered magnetic susceptibilities and possess high Weiss temperatures.

The unperturbed staggered susceptibility $\chi^{(0)}$ has been calculated numerically by Hotta[11] on the basis of the realistic d-p model. Figure 3(c) in Ref. 11 shows that

$$\partial[\chi^{(0)}]^{-1}/\partial T \approx (0.42^{-1}-1)/0.1 \approx 13.8,$$

while in the case of this paper $\partial[\chi]^{-1}/\partial T \approx 11.9$ according to the estimate (19). Thus, the Curie constant from the scaling calculations has also a reasonable value.

VI. CONCLUSION

A. Results

This paper shows that the multiplicative renormalization theory can be applied to the 2D problem where double logarithmic terms occur and how this theory can be brought further in order to find the temperature dependence of the magnetic susceptibility in LSCO.

The purpose was to study to what extent the existence of van Hove singularities can explain the physical behaviors in HTSC systems. The results from the scaling method seem to be in good correspondence with experiments, despite the fact that it strongly focuses on electron-electron correlation close to the van Hove singularities.

The scaling results can explain the expected Curie-Weiss temperature behavior of the staggered magnetic susceptibility in LSCO, with realistic Weiss temperatures in the range from 0 to 100 K, realistic values of $U/t=1\sim1.4$ and $1/5t \approx 10^{-4}$ K^{-1}. U/t is correctly decreasing when the dop-

ing is increased due to the increasing screening effect. The estimated Curie constant can be justified from numerical calculations.

It is hard to believe that the simple model of this paper alone can explain the complex high-temperature superconductor (HTSC) systems. However, the results of this paper strongly suggest that the van Hove singularities play an important role in HTSC systems, especially in LSCO.

The cutoff factor μ was also introduced. (This paper assumed that this cutoff factor stems from the chemical potential. This gives a qualitatively good explanation of experimental results but is not a main point in this paper.) Since this cutoff factor μ is large in the heavily doped materials YBCO and TBCO, the (T_1T)=const behavior can be observed. On the contrary, the Curie-Weiss behavior in the lightly doped LSCO appears due to the low value of the cutoff factor μ (chemical potential). The instability in the undoped and lightly doped LSCO systems occurs for the same reason.

However, it was only in the low-temperature region and for high correlation values that the scaling approach was an obvious improvement compared to the naive RPA expression. The advantage of the scaling approach which is to take higher-order electron-electron and electron-hole contributions into account was not fully used in this problem, since the main contribution turned out to be the ladder diagrams.

B. Further developments

The estimates and discussions in this paper have been quite rough. It is clear that the results need further investigation. It is of particular interest to explore the validity of the square-logarithmic parquet approximation and the similarity between the scaling results and the RPA result. It can also be useful to examine in more detail the effects of a nonzero chemical potential at low temperatures.

Better results can be obtained by going beyond the parquet approximation. For this purpose, a second-order scaling approach may be attempted even if it seems to be difficult. However, as the parquet approximation fails, it is probable that also the nonlogarithmic terms must be taken into account.

Apart from the scaling approach, the only known and reliable approach is high-order perturbational calculations with the d-p model. So far, numerical calculations only up to third order have been done by some authors.[12]

By perturbational calculations which take all diagram contributions into account, the foundation of the multiplicative renormalization theory can also be studied in detail. So far, the scaling approach in the 2D problem can be justified only by comparison with experimental results or with results from other approaches.

ACKNOWLEDGMENTS

The authors would like to express their sincere thanks to Professor S. Inagaki and Dr. S. Fujimoto for valuable discussions.

*Also at Norwegian Institute of Technology (NTH), Trondheim, Norway. Present address: Humleveien 12 N-0870 Oslo 8, Norway.

[1] H. J. Schulz, Europhys. Lett. **4**, 609 (1987).

[2] I. E. Dzyaloshinskii, Pis'ma Zh. Éksp. Theor. Fiz. **46**, 110 (1987) [JETP Lett. **46**, Suppl. 93 (1987)].

[3] H. Kohno and K. Yamada, Prog. Theor. Phys. **85**, 13 (1991).

[4] P. W. Anderson, J. Phys. C **3**, 2436 (1970).

[5] N. N. Bogoliubov and D. V. Shirkov, *Introduction to the Theory of Quantized Fields*, 3rd ed. (Wiley, New York, 1980).

[6] J. Solyom, Adv. Phys. **28**, 201 (1979).

[7] N. Menyhard and J. Solyom, J. Low Temp. Phys. **12**, 529 (1973); M. Fowler and A. Zawadowski, Solid State Commun. **9**, 471 (1971); M. Kimura, Prog. Theor. Phys. **53**, 955 (1974).

[8] Y. Kitaoka, K. Ishida, S. Ohsugi, K. Fujiwara, and K. Asayama, Physica C **185-189**, 98 (1991).

[9] T. Moriya, Y. Takahashi, and K. Ueda, J. Phys. Soc. Jpn. **59**, 2905 (1990); A. J. Millis, H. Monien, and D. Pines, Phys. Rev. **42**, 167 (1990); N. Bulut, D. Hone, D. J. Scalapino, and N. E. Bickers, Phys. Rev. **41**, 1797 (1990).

[10] G. Shirane, Y. Endoh, R. J. Birgeneau, M. A. Kastner, Y. Hidaka, M. Oda, M. Suzuki, and M. Murakami, Phys. Rev. Lett. **59**, 1613 (1987).

[11] T. Hotta, J. Phys. Soc. Jpn. **62**, 4414 (1993).

[12] T. Hotta, J. Phys. Soc. Jpn. **63**, 4126 (1994); D. J. Scalapino, E. Loh, Jr., and J. E. Hirsch, Phys. Rev. B **34**, 8190 (1986).